# Instabilities, defects, and defect ordering in an overdamped active nematic

Elias Putzig,[1, *] Gabriel S. Redner,[1, †] Arvind Baskaran,[2, ‡] and Aparna Baskaran[1, §]

[1]*Martin Fisher School of Physics, Brandeis University, Waltham, MA 02453, USA*
[2]*Department of Chemistry and Biochemistry,*
*University of Maryland, College Park, MD 20742, USA*
(Dated: June 12, 2015)

We consider a phenomenological continuum theory for an extensile, overdamped active nematic liquid crystal, applicable in the dense regime. Constructed from general principles, the theory is universal, with parameters independent of any particular microscopic realization. We show that it exhibits a bend instability similar to that seen in active suspensions, that leads to the proliferation of defects. We find three distinct nonequilibrium steady states: a defect-ordered nematic in which $+\frac{1}{2}$ disclinations develop polar ordering, an undulating nematic state with no defects, and a turbulent defective nematic. We characterize the phenomenology of these phases and identify the relationship of this theoretical description to experimental realizations and other theoretical models of active nematics.

Liquid crystals are anisotropic fluid mesophases that exhibit broken rotational symmetry and have been extensively studied and extremely useful for many years [1]. The study of topological defects in the orientational order in these systems, which typically occur under driving, has had a central role in developing our understanding of the material properties of these systems [2, 3]. Active liquid crystals are anisotropic fluid phases that are driven at the scale of the microscopic nematogen. These microscale internal forces give rise to spontaneous defect nucleation, and novel defect dynamics [4–6].

An experimental realization of a two-dimensional active nematic with rich phenomenology is a system of cytoskeletal filaments driven by motor proteins [4–6] confined to a fluid interface. This novel nonequilibrium system has been shown to have transient self-propelled defects and emergent defect ordering and has triggered much theoretical effort to understand its dynamics [6–18]. One outcome of the theories is to show how fluid mediation, in the form of active and passive backflow, can lead to the formation and propulsion of defects. However, defects also arise in active nematic systems in which fluid mediation plays little or no part, such as vibrated monolayers of granular rods [19], epithelial cell monolayers [20], and elongated fibroblasts [21].

In this work we develop a phenomenological continuum theory that describes the dynamics of an overdamped active nematic, and is applicable to all systems in this symmetry class in two dimensions. The nonequilibrium steady-states that we find are (i) a defect-ordered nematic that exhibits emergent polar ordering of $+\frac{1}{2}$ defects, (ii) a defect-free undulating nematic, and (iii) a defective, turbulent nematic (see Fig. 1). Further, we identify the relationship of existing theories to this framework.
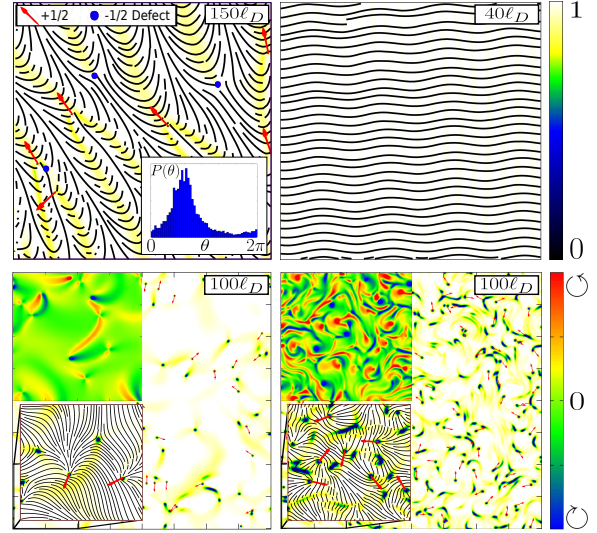


FIG. 1. (color online) Heatmaps of the degree of order ($S/S_0$, colorbar on the upper-right) showing the nonequilibrium steady-states. Top Left Panel: The defect-ordered state, with a histogram inset showing the sharp polar ordering in the orientation of $+\frac{1}{2}$ defects. The lines, showing the direction of order, highlight the extended trails left by the motion of these defects. Top Right Panel: The undulating nematic state is highly ordered ($S \simeq S_0$) but the direction of order undulates. Bottom Panels: Defective states at low activity (left, $\psi < 1$) and high activity (right, $\psi > 1$), with 2×-magnified regions (lower left), and heatmaps of the vorticity (in the upper left, colorbar on the lower-right). Scale bars are on the top right.

**Theoretical Framework**: An equilibrium nematic is described by the well-known Landau-de Gennes free energy that is a functional of the density $\rho(\vec{r}, t)$ and the nematic order tensor, $\mathbf{Q}(\vec{r}, t)$, associated with rotational symmetry breaking [1]. Its

dynamics is given by gradient descent on this free energy landscape: 'Model A' dynamics for the director, $\partial_t \mathbf{Q}(\vec{r}) = -\gamma^{-1} \frac{\delta F}{\delta \mathbf{Q}(\vec{r})}$, and 'Model B' dynamics for the density, $\partial_t \rho(\vec{r}) = -\gamma'^{-1} \nabla^2 \frac{\delta F}{\delta \rho(\vec{r})}$, as density is conserved. If this system is in an imposed flow then the director is convected and rotated by that flow, and the dynamical equation becomes

$$(\partial_t + \vec{u} \cdot \vec{\nabla})\mathbf{Q} = -\gamma^{-1} \frac{\delta F}{\delta \mathbf{Q}} + \mathbf{Q}\mathbf{\Omega} - \mathbf{\Omega}\mathbf{Q}$$
$$+ \lambda \mathbf{E} + \lambda(\mathbf{Q}\mathbf{E} + \mathbf{E}\mathbf{Q})^{\mathcal{T}}$$

where $\mathbf{\Omega}$ is the vorticity tensor, $\mathbf{E}$ is the strain-rate tensor associated with the flow, $\lambda$ is the flow-alignment parameter, and $(\mathbf{A})^{\mathcal{T}}$ denotes the traceless version of $\mathbf{A}$ (e.g. $\mathbf{A} - \frac{1}{2}Tr(\mathbf{A})\mathbf{I}$).

In the case of an active liquid crystal, internal stresses due to the forces exerted by the particles themselves give rise to self-generated flows. We *postulate* that an active liquid crystal undergoes gradient descent dynamics in the local rest frame of this *self-generated flow arising from the activity*. The active stress has the same symmetry as the nematic order ($\sigma \propto \mathbf{Q}$) and hence the self-generated flow will be proportional to the force density: $\rho\vec{u} = \vec{F}/\xi_T \equiv -\lambda_C \vec{\nabla}\mathbf{Q}$. Similarly the vorticity will be proportional to the torque density: $\rho\vec{\omega} = \vec{\tau}/\xi_R \equiv \lambda_R(\vec{\nabla} \times \vec{\nabla}\mathbf{Q})$, where $\xi$'s denote friction coefficients. Using the form of the flow and vorticity arising from the activity, the dynamical equations for an active nematic take the form

$$\partial_t \mathbf{Q} = -\gamma^{-1} \frac{\delta F}{\delta \mathbf{Q}} + \frac{\lambda_C}{\rho}[\vec{\nabla}\mathbf{Q}] \cdot \vec{\nabla}\mathbf{Q} - \frac{\lambda_S}{2\rho}\mathbf{Q}(\boldsymbol{\nabla}\boldsymbol{\nabla} : \mathbf{Q})$$
$$- \frac{\lambda_R}{\rho}\left(\mathbf{Q} \cdot \boldsymbol{\nabla}\boldsymbol{\nabla} \cdot \mathbf{Q} - \vec{\nabla}(\vec{\nabla}\mathbf{Q}) \cdot \mathbf{Q}\right)^{\mathcal{S}} \qquad (1)$$

where the coefficients $\lambda_C$, $\lambda_R$, and $\lambda_S$ control the strength of active convection, active torque, and flow-alignment respectively, $\mathbf{A} : \mathbf{B} = A_{ij}B_{ij}$, and $\mathcal{S}$ denotes symmetrization (e.g. $\left(\mathbf{A}\right)^{\mathcal{S}} = \frac{1}{2}(\mathbf{A} + \mathbf{A}^{\mathbf{T}})$). Further, we take the dynamics of the density to be of the form

$$\partial_t \rho = D\nabla^2 \rho + D_Q \boldsymbol{\nabla}\boldsymbol{\nabla} : \mathbf{Q} \qquad (2)$$

which incorporates the self-generated flow through the curvature induced density flux [22, 23], controlled by $D_Q$.

Equations (1) and (2) are the dynamical equations of an overdamped active nematic which will be studied in this work. Before we proceed with the analysis of our theory, we make the following observations in

order to place this model in the context of other theories in the literature of active liquid crystals:

(1) Suppose our active fluid had polar symmetry, the self generated flow will be proportional to the polar order parameter, $\rho\vec{u} = \vec{F}/\xi_T \equiv \lambda\vec{P}$. Postulating a gradient descent dynamics, as above, for an active polar fluid results in the same dynamics as described in the seminal works of Toner and Tu [24, 25]. In this sense, this theory is a generalization of their approach to active nematic systems.

(2) Existing theories of active nematics consider a coupled set of equations of the nematic order parameter and the active induced flow which arises from a Stokes equation (such as [7–13, 18]). Suppose there exists a screening mechanism such as confinement to 2D, then eliminating the flow field in terms of the active stress yields Eqs (1) and (2) above, but with $\lambda_C = \lambda_R$ i.e., a Galilean invariant version of our theory [18, 26–28]. This is an important distinction of our work. In overdamped systems Galilean invariance is broken by the medium through which our particles move (as first pointed out in [24]) and this is accounted for in our theory.

(3) Theoretical work on active nematics was pioneered in [22, 23], and have subsequently been shown to have giant number fluctuations, phase separation, and band formation near the critical density [19, 29–40]. Our Eqs (1) and (2) reduce to this description when $\lambda_R = \lambda_C = \lambda_S = 0$. Hence our theory can be considered a generalization of these previous works.

**Parameters of the theory**: The equilibrium contributions to the dynamics of the order parameter take the form

$$[\partial_t Q_{ij}]_{Eq} = D_r[\alpha - \beta Tr\mathbf{Q}^2]Q_{ij} + 2D_E \nabla^2 Q_{ij}$$
$$+ \frac{D_\delta}{\rho}\left(2\partial_k(Q_{kl}\partial_l Q_{ij}) - ([\partial_i Q_{kl}]\partial_j Q_{kl})^{\mathcal{T}}\right)$$
$$+ D_\rho(\partial_i \partial_j)^{\mathcal{T}}\rho - K\nabla^4 Q_{ij}$$

where $\alpha = (\rho - 1)$ and $\beta = \frac{1}{\rho^2}(\rho + 1)$. $D_r$ is the rotational diffusion constant and $D_\rho$ is a kinetic term also seen in prior works [31, 32, 36]. There are two elastic terms; $D_E$ is a mean elasticity, and $D_\delta$ is a differential elasticity, measuring the difference between bend and splay energies. Finally, a fourth-order gradient term (with coefficient $K$) is included in order to ensure smoothness and numerical stability. The relevant parameters for the phenomenology discussed are: the active force and torque ($\lambda_{C,R}$) and the differential elastic constant $D_\delta$. In the following, we non-dimensionalize our equations by setting our time scale to be the rotational diffusion time, $\frac{1}{D_r}$, and our length-scale to be the diffusion length,

$\ell_D \equiv \sqrt{D/D_r}$. In all of the subsequent sections we will work in these dimensionless variables.

**Instabilities of the Nematic State**: In the homogeneous limit, Eqs. (1) and (2) admit a uni-axial nematic solution with average density $\rho_0 > 1$, and the order parameter $\mathbf{Q} = \rho_0 S_0(\hat{\boldsymbol{x}}\hat{\boldsymbol{x}} - \frac{1}{2}\mathbf{I})$ with $S_0 = \sqrt{\frac{2(\rho_0-1)}{\rho_0+1}}$. Let us consider spatial fluctuations about this state.

Fluctuations perpendicular to the director cause an instability when $D_Q > \sqrt{2(\rho_0^2-1)}\left(\frac{\rho_0+1}{\rho_0^2+\rho_0-1}\right)$. This instability causes phase separation into bands of dense ordered regions coexisting with dilute disordered regions when the material is near the critical density ($\rho_c = 1$). This has been discussed in previous work by us [40] and others [34–36, 38, 39]. The nonlinear active terms ($\lambda_C$, $\lambda_R$ and $\lambda_S$) do not alter the instability, nor do they significantly alter the phenomenology discussed in previous work.

Of primary interest here is a bend instability in which the direction of ordering is destabilized by fluctuations parallel to the director. This occurs when a 'bend instability parameter' $\psi > 1$, where $\psi = \frac{\lambda_R - 2D_\delta}{D_E \cdot \Lambda(\rho_0)}$, and $\Lambda(\rho_0) = 4\sqrt{\frac{\rho_0+1}{2(\rho_0-1)}}$. This instability parameter reflects a competition between the active torque $\lambda_R$ and the differential elastic constant $D_\delta$, which is positive if the energetic cost to bend distortions of the director is greater than that of splay. The bend instability is the primary mechanism for defect generation and formation of inhomogeneous steady states in this active system.

In order to elucidate the consequence of this bend instability, we numerically explored the dynamics using a semi-implicit finite difference method, with periodic boundary conditions. Integrating from nematic initial conditions with small amplitude Gaussian noise, two states were found above the bend instability ($\psi > 1$). These were (I) an undulating nematic state (see Fig. 2) where the system is strongly ordered but the director undulates along the broken symmetry direction (see Fig. 1), and (II) a turbulent state (see Fig. 2,1) in which charge $\pm\frac{1}{2}$ disclinations continually form and annihilate and the $+\frac{1}{2}$ defects are self-propelled as seen in [4–15]. The undulating nematic state was present when active convection $\lambda_C > 1.0$ and when $D_\delta \preceq 0$. In other regions of parameter space the system transitioned directly into the defective nematic state. [41]

The above analysis focused on the instabilities of the homogeneous nematic state. Next we consider isotropic initial conditions and present the results for different values of the parameters that control the bend instability ($\lambda_R$, $D_\delta$, and $\rho_0$) while keeping the
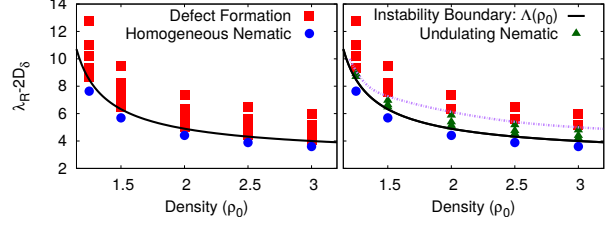


FIG. 2. (color online) Plots showing the end state which forms from nematic initial conditions. Left: At $D_\delta = 1.0$, the homogeneous nematic state transitions into a defective nematic. Right: At $D_\delta = -0.50$ we find an undulating state at intermediate activities.
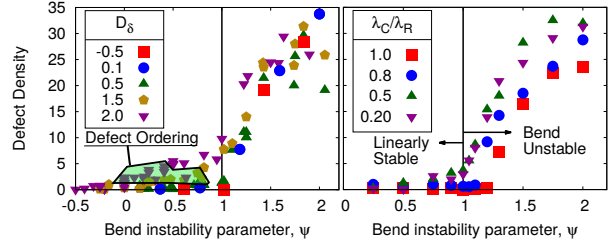


FIG. 3. (color online) Plots of the defect density $n$ (defects per $(100\ell_D)^2$) as a function of $\psi$. Left: Curves with fixed $\lambda_C = 1.0$, a range of $D_\delta$ and $\rho_0$ (scaled as $n/(\rho_0-1)$). Defect density is greater for larger $D_\delta$ when $\psi < 1$, increases sharply when $\psi$ crosses 1, then saturates. The shaded region indicates where there was statistically significant polar ordering of $+\frac{1}{2}$ defects. Right: Fixed $D_\delta = 1.0$, for a range of $\lambda_C/\lambda_R$, shows that when the active convection is comparable to active torque, defects vanish near the bend instability.

other parameters fixed ($\lambda_C = D_\rho = D_E = D = 1.0$, $K = 0.50$, $\lambda_S = 0$, and $D_Q = 0.10$) unless otherwise specified.

**Defect-ordered state**: This nonequilibrium steady state occurs when defects form below the bend instability ($\psi < 1$). This occurs when the strength of active torque is dominant over the strength of active convection (see Fig. 3). The properties of this state are as follows: (i) Defects are point-like and the background is a well-ordered nematic (see Fig. 1). (ii) Defining the orientation of $+\frac{1}{2}$ defects to be opposite the "comet tail" (along the direction of propulsion), we find that these defects exhibit *significant polar ordering*. (iii) The degree of polar ordering decreases as $\psi$ increases. (iv) The high degree of polar ordering corresponds with long splay distortions which are left by $+\frac{1}{2}$ defects as they travel (see Fig. 1). Other $+\frac{1}{2}$ defects tend to reorient rather than cross this distortion-trail, leading to long parallel structures which are visible in the states with a large degree of polar ordering.
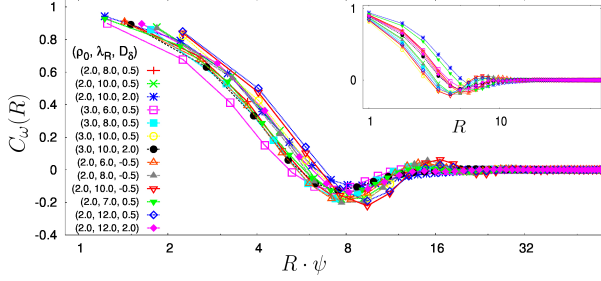
FIG. 4. (color online) Log-linear plot of vorticity correlation functions, $C_\omega(R)$ for fixed parameters ($\lambda_R$, $D_\delta$ and $\rho_0$) above the bend instability ($\psi > 1.10$). The length is scaled by $\psi$, which gives a data collapse for a large range of parameters.

**Turbulent nematic state**: The turbulent, defective nematic state occurs just above the bend instability and has the following properties: (i) Defect density and vorticity increase sharply for $\psi \sim 1$. (ii) There is a saturation, or even a decrease, in the defect density (see Fig. 3) as the defects, which were point-like and circular near $\psi = 1$, become spatially extended and the average degree of ordering decreases. (iii) The vorticity correlation function $C_\omega(R) = \langle \omega(0)\omega(R)\rangle / \langle \omega^2 \rangle$, scales with the bend instability parameter $\psi$ (see Fig 4), which is linear in the strength of the active torque $\lambda_R$. This differs from what was found in a fluid-mediated active nematic theory [12] where vorticity scaled to the 1/4th power of the strength of the activity. (iv) Assuming that the length scale for defect separation $\ell_d$ scales with the vorticity ($\ell_d \propto \frac{1}{\psi}$) would lead to a prediction that defect density scales as $\psi^2$. This seems compatible with the trend seen near the critical value of the bend instability parameter, but the range is not large enough for a conclusive comparison.

**Discussion**: We have introduced a universal model of an overdamped active nematic in which activity enters through self-induced flows. This theory encompasses existing work on active nematics as special cases. The active torque from self-generated flows gives rise to a bend instability which, in turn, leads to defect formation. We have identified three nonequilibrium steady states admitted by this theory. The first is a defect-ordered nematic state where polar ordering of +1/2 disclinations emerges from the underlying apolar theory. The second is an undulating nematic state which is reminiscent of the "walls" of distortion in the order parameter seen before the onset of defective states [10, 12], or the distortion of the director which happens during relaxation oscillations [42, 43] in active nematic sus-

pensions. Finally we find a turbulent nematic state similar to that which occurs in theories of active nematic suspension [7–13].

The appearance of a defect-ordered state is of particular interest, as defect-ordering was recently discovered in layers of active cytoskeletal filaments and in simulations of that system [6]. Our theory provides robust predictions about when defect ordering will be found. The ordering occurs below the bend instability, i.e., $\psi < 1$, and only for $D_\delta > 0$, which indicates that the energetic penalty to bend distortions must be greater than that of splay, and the strength of the active torque must be greater than that of the active convection. This result implies that an orientationally ordered fluid phase of defects may not occur in theories which have Galilean invariance ($\lambda_C = \lambda_R$).

In [6], defect ordering in the experiment had nematic symmetry, while simulations displayed the same polar symmetry that we observe. This may be due to the use of periodic boundary conditions in both the simulations in [6] and our work, or the nematic ordering could be a subtle effect of fluid-mediated interactions in the experiment. However, the strong similarities between this theory and the experimental system, such as the sharp splay distortions left in the wake of traveling $+\frac{1}{2}$ defects leads us to believe that the parameter space in which this system operates is $\psi < 1$, $\lambda_C < \lambda_R$ and $D_\delta > 0$. Further work is needed to substantiate this in detail.

The theory that we have described contains a rich and diverse phenomenology which overlaps with other theories, simulations, and experiments of active nematics. It is generic and universal in that it is independent of any particular microscopic model and only relies on the nematic having local interactions.

* efputzig@brandeis.edu
† gredner@brandeis.edu
‡ baskaran@math.uci.edu
§ aparna@brandeis.edu

[1] P.-G. De Gennes and J. Prost, *The physics of liquid crystals*, Vol. 23 (Clarendon press Oxford, 1993).

[2] P. M. Chaikin and T. C. Lubensky, *Principles of condensed matter physics*, Vol. 1 (Cambridge Univ Press, 2000).

[3] O. D. Laverntovich, *Soft matter physics: an introduction* (Springer Science & Business Media, 2003).

[4] T. Sanchez, D. T. N. Chen, S. J. DeCamp, M. Heymann, and Z. Dogic, Nature , 24 (2013), 1301.1122.

[5] F. C. Keber, E. Loiseau, T. Sanchez, S. J. DeCamp, L. Giomi, M. J. Bowick, M. C. Marchetti, Z. Dogic, and A. R. Bausch, Science **345**, 1 (2014).

[6] S. J. Decamp, G. S. Redner, A. Baskaran, M. F. Hagan, and Z. Dogic, arXiv.org , 1 (2015), arXiv:arXiv:1501.06228v2.

[7] L. Giomi, M. J. Bowick, X. Ma, and M. C. Marchetti, Phys. Rev. Lett. **110**, 228101 (2013).

[8] S. P. Thampi, R. Golestanian, and J. M. Yeomans, Phys. Rev. Lett **111**, 118101 (2013).

[9] M. L. Blow, S. P. Thampi, and J. M. Yeomans, Phys. Rev. Lett. **113**, 248303 (2014).

[10] L. Giomi, M. J. Bowick, P. Mishra, R. Sknepnek, and M. C. Marchetti, Philosophical Transactions of the Royal Society A: Mathematical, Physical and Engineering Sciences **372**, 20130365 (2014).

[11] S. P. Thampi, R. Golestanian, and J. M. Yeomans, Physical Review E **90**, 062307 (2014).

[12] S. P. Thampi, R. Golestanian, and J. M. Yeomans, Philosophical Transactions of the Royal Society A: Mathematical, Physical and Engineering Sciences **372**, 20130366 (2014).

[13] S. P. Thampi, R. Golestanian, and J. M. Yeomans, EPL (Europhysics Letters) **105**, 18001 (2014).

[14] T. Gao, R. Blackwell, M. A. Glaser, M. Betterton, and M. J. Shelley, Physical review letters **114**, 048101 (2015).

[15] X.-q. Shi and Y.-q. Ma, Nat. Commun. **4**, 3013 (2013).

[16] D. Saintillan and M. J. Shelley, Physical Review Letters **99**, 1 (2007).

[17] D. Saintillan and M. J. Shelley, Physical Review Letters **100**, 1 (2008).

[18] A. Doostmohammadi, M. Adamer, S. P. Thampi, and J. M. Yeomans, arXiv.org , 1 (2015), arXiv:arXiv:1505.04199v1.

[19] V. Narayan, S. Ramaswamy, and N. Menon, Science **317**, 105 (2007).

[20] R. Kemkemer, D. Kling, D. Kaufmann, and H. Gruler, Eur. Phys. J. E **1**, 215 (2000).

[21] G. Duclos, S. Garcia, H. G. Yevick, and P. Silberzan, Soft matter **10**, 2346 (2014).

[22] R. Simha and S. Ramaswamy, Physica A: Statistical Mechanics and its Applications **306**, 262 (2002).

[23] S. Ramaswamy, R. A. Simha, and J. Toner, Europhys. Lett. **62**, 196 (2003).

[24] J. Toner and Y. Tu, Phys. Rev. Lett. **75**, 4326 (1995).

[25] J. Toner and Y. Tu, Phys. Rev. E **58**, 4828 (1998).

[26] L. M. Pismen, Phys. Rev. E **88**, 050502 (2013).

[27] P. Srivastava and M. C. Marchetti, Private Commnication (2015).

[28] P. Srivastava and M. C. Marchetti, "Instabilities and patterns in an active nematic film," APS March Meeting (2015).

[29] S. Mishra and S. Ramaswamy, Phys. Rev. Lett **97**, 090602 (2006).

[30] H. Chaté, F. Ginelli, and R. Montagne, Phys. Rev. Lett **96**, 180602 (2006).

[31] A. Baskaran and M. C. Marchetti, Physical Review E **77**, 011920 (2008).

[32] A. Baskaran and M. Marchetti, Phys. Rev. Lett **101**, 268101 (2008).

[33] S. Mishra, R. Aditi Simha, and S. Ramaswamy, J. Stat. Mech. Theory Exp. **2010**, P02003 (2010).

[34] F. Peruani, F. Ginelli, M. Bär, and H. Chaté, J. Phys. Conf. Ser. **297**, 012014 (2011).

[35] A. Peshkov, S. Ngo, E. Bertin, H. Chaté, and F. Ginelli, Phys. Rev. Lett. **109**, 098101 (2012).

[36] A. Peshkov, I. S. Aranson, E. Bertin, H. Chaté, and F. Ginelli, Phys. Rev. Lett. **109**, 268701 (2012).

[37] A. Baskaran and M. C. Marchetti, Eur. Phys. J. E. **35**, 95 (2012).

[38] E. Bertin, H. Chaté, F. Ginelli, S. Mishra, A. Peshkov, and S. Ramaswamy, New J. Phys. **15**, 085032 (2013).

[39] S. Ngo, A. Peshkov, I. S. Aranson, E. Bertin, F. Ginelli, and H. Chaté, Physical Review Letters , 038302 (2013), 1312.1076.

[40] E. Putzig and A. Baskaran, Physical Review E **90**, 042304 (2014), 1057984.

[41] Details of the this transition, as well as the additional discussion concerning the equations and linear stability analysis, can be found in the supplement.

[42] L. Giomi, L. Mahadevan, B. Chakraborty, and M. F. Hagan, Phys. Rev. Lett. **106**, 218101 (2011).

[43] L. Giomi, L. Mahadevan, B. Chakraborty, and M. F. Hagan, Nonlinearity , 2245 (2012).

# Supplementary Information
## (Instabilities, defects, and defect ordering in an overdamped active nematic)

Elias Putzig,[1, *] Gabriel S. Redner,[1, †] Arvind Baskaran,[2, ‡] and Aparna Baskaran[1, §]

[1] *Martin Fisher School of Physics, Brandeis University, Waltham, MA 02453, USA*
[2] *Department of Chemistry and Biochemistry,*
*University of Maryland, College Park, MD 20742, USA*

* efputzig@brandeis.edu
† gredner@brandeis.edu
‡ baskaran@math.uci.edu
§ aparna@brandeis.edu

## I.  FREE ENERGY

The dynamics of an equilibrium liquid crystal, which were discussed in the body of the text, can be derived from gradient descent on the well-known Landau-de Gennes free energy [1]:

$$F = \int d^d r \Big[ -\frac{\alpha}{2} Tr(\mathbf{Q}^2) + \frac{\beta}{4}\big(Tr(\mathbf{Q}^2)\big)^2 + \chi Q_{ij}\partial_i\partial_j\rho + \frac{1}{2}\kappa Q_{ij}\nabla^4 Q_{ij}$$
$$+ \frac{1}{2}L_1(\partial_i Q_{kl})^2 + \frac{1}{2}L_2(\partial_i Q_{ik})\partial_j Q_{jk} + \frac{1}{2\rho}L_4 Q_{ij}(\partial_i Q_{kl})\partial_j Q_{kl} \Big] + \Phi[\rho] \tag{1}$$

where the homogeneous terms give a second order phase transition and the terms with coefficients $L_i$ are elastic terms, associated with the energy cost of director distortions. The elastic energy cost is widely described in terms of splay $(K_{11}(\nabla \cdot \hat{n})^2)$ and bend $\big(K_{33}\big(\hat{n} \times (\nabla \times \hat{n})\big)^2\big)$ distortion of the director. The parameters in (1) are related to the splay and bend coefficients as: $K_{11} = S^2(2L_1 + L_2 - SL_4)$ and $K_{33} = S^2(2L_1 + L_2 + 2SL_4)$.

The gradient-descent dynamics from the body of the paper came from taking a derivative of Eq. 1:

$$-\gamma^{-1}\frac{\delta F}{\delta Q_{ij}} = D_r[\alpha - \beta Tr\mathbf{Q}^2]Q_{ij} + 2D_E\nabla^2 Q_{ij} + D_\rho(\partial_i\partial_j - \frac{1}{2}\delta_{ij}\nabla^2)\rho - K\nabla^4 Q_{ij}$$
$$+ \frac{D_\delta}{\rho}\Big(2Q_{kl}\partial_k\partial_l Q_{ij} + 2[\partial_k Q_{kl}]\partial_l Q_{ij} - \big([\partial_i Q_{kl}]\partial_j Q_{kl} - \frac{1}{2}\delta_{ij}[\partial_k Q_{lm}]^2\big)\Big)$$

where $D_r = 2/\gamma$, $D_\rho = -2\chi/\gamma$, $K = 2\kappa/\gamma$ and the two mean elastic terms have been consolidated by using the tracelessness and symmetry of $Q$ to group them in the term with coefficient $D_E = 2L_1/\gamma = 2L_2/\gamma$. The differential elastic coefficient, $D_\delta = 2L_4/\gamma$, has a range $-\frac{3}{2S} < \frac{D_\delta}{D_E} < \frac{3}{S}$, and is set by the requirement that the equilibrium nematic should be stable to director fluctuations. Further a fourth order gradient term (with coefficient $K$) is included in order to ensure smoothness and numerical stability.

## II.  ACTIVE STRESSES AND SELF-INDUCED FLOWS

In the body of the text we considered the dynamics of the director when the system was in an imposed flow, in which case the dynamical equation becomes

$$(\partial_t + \vec{u}\cdot\vec{\nabla})Q_{ij} = -\gamma^{-1}\frac{\delta F}{\delta Q_{ij}} + (Q_{ik}\Omega_{kj} - \Omega_{ik}Q_{kj})$$
$$+ \lambda E_{ij}^{\mathcal{T}} + \lambda(Q_{ik}E_{kj} + E_{ik}Q_{kj})^{\mathcal{T}}$$

where $\Omega_{ij}$ and $E_{ij}$ are the vorticity and strain-rate tensor associated with the flow, and $\lambda$ is the flow-alignment parameter. We then postulated a form for the self-generated flow $\rho\vec{u} = -\lambda_C\vec{\nabla}\mathbf{Q}$, and the vorticity $\rho\vec{\omega} = \lambda_R(\vec{\nabla}\times\vec{\nabla}\mathbf{Q})$. This is consistent with a stress proportional to the nematic order, $\boldsymbol{\sigma} = \sigma_a\mathbf{Q}$ where coefficients $(\sigma_a, \lambda_C$ and $\lambda_R)$ are positive for systems of extensile, 'pusher' particles, and negative for contractile, 'puller' particles.

We construct the tensors $\Omega_{ij}$ and $E_{ij}$ in a straightforward manner from these flows. The z- component of the vorticity vector gives the amount that a fluid element is rotated by the self-generated flow in two dimensions, and the vorticity tensor, which comes into the dynamics, is $\rho\Omega_{ij} = \frac{1}{2}\epsilon_{ijk}\omega_k$ where $\epsilon$ is the Levi-Civita symbol. The strain-rate tensor, which is the symmetrized gradient of the flow $E_{ij} = \frac{1}{2}(\partial_i u_j - \partial_j u_i)$ will play a role if the particles tend to align or tumble in shear.

We postulated that an active liquid crystal undergoes gradient descent dynamics so as to minimize the energy cost of director distortions and inhomogeneities, in the local rest frame of this self-generated flow arising from the activity. Using the form of the flow and vorticity arising from the activity identified above,

our dynamical equations for an active nematic take the form

$$\partial_t Q_{ij} = -\gamma^{-1}\frac{\delta F}{\delta Q_{ij}} + \frac{\lambda_C}{\rho}[\partial_k Q_{kl}]\partial_l Q_{ij} - \frac{\lambda_S}{2\rho}Q_{ij}\partial_k\partial_l Q_{kl} \tag{2}$$

$$-\frac{\lambda_R}{2\rho}\big(Q_{ik}\partial_k\partial_l Q_{jl} - Q_{ik}\partial_j\partial_l Q_{kl} - Q_{kj}\partial_i\partial_l Q_{kl} + Q_{kj}\partial_k\partial_l Q_{il}\big)$$

where $\lambda_S = \lambda\lambda_C$ is the strength of flow-alignment, and we have simplified the flow-alignment term in the expression above using the symmetry and tracelessness of the nematic order tensor.

The form of the flow-alignment term in this overdamped case is different from the form that arises in the overdamped limit of the the theories in which flow arises through a Stokes equation (such as [2–8]). This is because the phenomenological, overdamped theory which we consider here does not have incompressible flows. Because of this, the first order flow-alignment term in the gradient descent dynamics ($\lambda E_{ij}^{\mathcal{T}}$) is not intrinsically traceless and must be made so by hand in order to preserve the symmetric and traceless nature of $\mathbf{Q}$, and the second order term ($\lambda(Q_{ik}E_{kj} + E_{ik}Q_{kj})^{\mathcal{T}}$) is nonzero, whereas it is zero in two dimensions for incompressible flow. The traceless version of the first order flow-alignment term is included in the functional derivative in Eq. 2, as it is the same as the mean elastic term: $E_{ij}^{\mathcal{T}} = \partial_k(\partial_i Q_{kj} + \partial_j Q_{ik} - \delta_{ij}\partial_l Q_{kl}) = \nabla^2 Q_{ij}$.

## III.   LINEAR STABILITY

In the homogeneous limit, Eq. (2) and the dynamical equation for the density, $\partial_t\rho = D\nabla^2\rho + D_Q\boldsymbol{\nabla\nabla} : \mathbf{Q}$, admit a homogeneous uni-axial nematic state with average density $\rho_0 > 1$, and the order parameter $\mathbf{Q} = \rho_0 S_0(\hat{\boldsymbol{x}}\hat{\boldsymbol{x}} - \frac{1}{2}\mathbf{I})$ with $S_0 = \sqrt{\frac{2(\rho_0-1)}{\rho_0+1}}$. Without loss of generality, we have picked coordinates so that the direction of nematic ordering is along the $x$-axis of our coordinate system. We parameterize the fluctuations about this state in the form $\rho(\mathbf{r},t) = \rho_0 + \delta\rho(\mathbf{r},t)$, $Q_{xx}(\mathbf{r},t) = \frac{1}{2}\rho_0 S_0 + \delta Q_{xx}(\mathbf{r},t)$ and $Q_{xy}(\mathbf{r},t) = \delta Q_{xy}(\mathbf{r},t)$. Further, we introduce a Fourier transform $\tilde{X} = \int d\mathbf{r}e^{i\mathbf{k}\cdot\mathbf{r}}X(\mathbf{r},t)$. The resulting linearized equations in Fourier space are

$$\partial_t\delta\tilde{\rho} = -Dk^2\delta\tilde{\rho} - D_Q k^2\cos(2\phi)\delta\tilde{Q}_{xx} - D_Q k^2\sin(2\phi)\delta\tilde{Q}_{xy} \tag{3a}$$

$$\begin{aligned}
\partial_t\delta\tilde{Q}_{xx} = &\ \Big(C_0 - \tfrac{1}{2}D_\rho k^2\cos(2\phi)\Big)\delta\tilde{\rho} \\
&- \Big(2\alpha_0 + 2D_E k^2 + (D_\delta - \tfrac{1}{2}\lambda_S)S_0 k^2\cos(2\phi) + Kk^4\Big)\delta\tilde{Q}_{xx} \\
&+ \tfrac{1}{2}\lambda_S S_0 k^2\sin(2\phi)\delta\tilde{Q}_{xy}
\end{aligned} \tag{3b}$$

$$\begin{aligned}
\partial_t\delta\tilde{Q}_{xy} = &- \tfrac{1}{2}D_\rho k^2\sin(2\phi)\delta\tilde{\rho} \\
&- \tfrac{\lambda_R}{2}S_0 k^2\sin(2\phi)\delta\tilde{Q}_{xx} \\
&- \Big(2D_E k^2 - \tfrac{\lambda_R}{2}S_0 k^2\cos(2\phi) + D_\delta S_0 k^2\cos(2\phi) + Kk^4\Big)\delta\tilde{Q}_{yx}
\end{aligned} \tag{3c}$$

where $\phi$ is the angle between the director (along the $x$ axis in our coordinates) and the spatial gradient vector $\mathbf{k}$. Also, we have defined parameters $C_0 = \sqrt{\frac{2(\rho_0-1)}{\rho_0+1}}\left(\frac{\rho_0^2+\rho_0-1}{\rho_0+1}\right)$, and $\alpha_0 = \rho_0 - 1$ for notational compactness.

The stability of these equations is best explicated by considering spatial fluctuations along ($\phi = 0$) or perpendicular to ($\phi = \frac{\pi}{2}$) the direction of ordering. In these two sectors, the fluctuations in the direction of ordering $\delta\tilde{Q}_{xy}$ decouple form those of the magnitude of ordering $\delta\tilde{Q}_{xx}$ and the density $\delta\tilde{\rho}$, thereby enabling a clear identification of mechanisms at play.

The decoupled dynamics of $\delta\tilde{Q}_{xy}$ are of the following form:

$$\partial_t\delta\tilde{Q}_{xy} = -\Big(2D_E(1\mp\psi)k^2 + Kk^4\Big)\delta\tilde{Q}_{xy} \tag{4}$$

where the coefficient of $k^2$ is proportional to $(1-\psi)$ for fluctuations along the director ($\phi = \frac{\pi}{2}$) and $(1+\psi)$ for fluctuations which are perpendicular ($\phi = 90°$). The stability parameter, which is useful for describing the

dynamics when bend in unstable, is $\psi = \frac{\lambda_R - 2D_\delta}{D_E \cdot \Lambda(\rho_0)}$, where $\Lambda(\rho_0) = 4\sqrt{\frac{\rho_0 + 1}{2(\rho_0 - 1)}}$. This instability is the primary mechanism for defect generation and formation of inhomogeneous steady states in this active system, as was discussed in the body of the paper.

Note that if the nematic was contractile, $\lambda_R$ is negative and hence there exists a splay instability, which occurs when $\psi < -1$. The analogous instability in fluid-mediated dynamics, which arises due to contractile stresses in the Stokes equation, has been studied in some detail [5, 7, 8]. This splay instability leads to defect formation, despite the fact that contractile systems enhance defect annihilation [2]. We have, however, focused on extensile systems for this study of the overdamped dynamics, and left the study of the contractile, overdamped dynamics to future work.

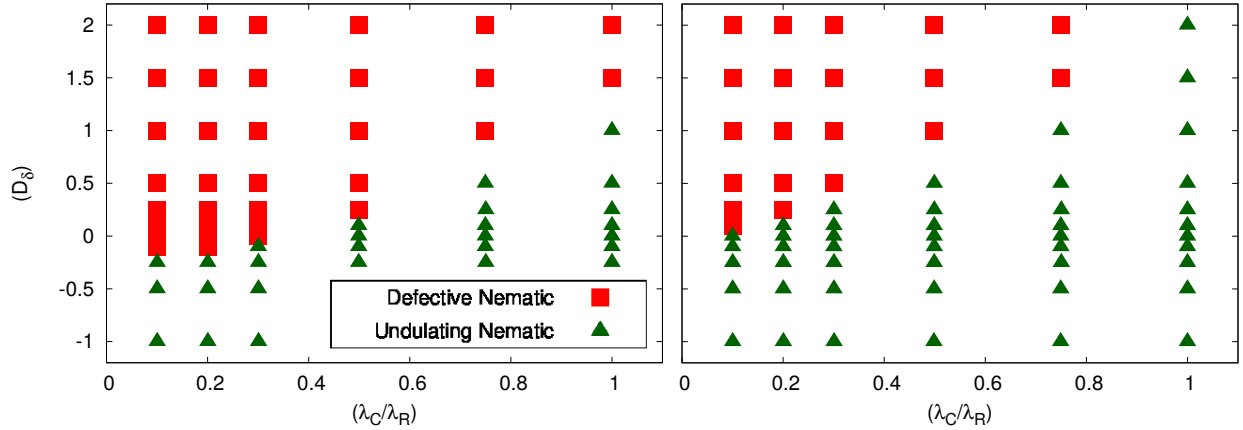## IV. ADDITIONAL NUMERICAL PHENOMENOLOGY



FIG. 1. These plots indicate whether an undulating nematic, or a turbulent, defective nematic state formed out of nematic initial conditions, from a point near the bend instability ($\psi = 1.05$, $\rho_0 = 2.0$). Left Panel: A flow-tumbling system, with $\lambda_S = -1.0$. Right Panel: A flow-aligning system with $\lambda_S = 1.0$. The formation of defects near the critical density is facilitated by having a strength of active convection which is small compared to the strength of the active torque ($\lambda_C/\lambda_R < 1$), and by a large energetic penalty to bend deformations, compared to the penalty to splay deformations ($D_\delta > 0$). Flow-tumbling systems also facilitate the formation of defects near the critical density, but flow-aligning versus flow-tumbling seems to be a small effect.

[1] P.-G. De Gennes and J. Prost, *The physics of liquid crystals*, Vol. 23 (Clarendon press Oxford, 1993).
[2] L. Giomi, M. J. Bowick, X. Ma, and M. C. Marchetti, Phys. Rev. Lett. **110**, 228101 (2013).
[3] S. P. Thampi, R. Golestanian, and J. M. Yeomans, Phys. Rev. Lett **111**, 118101 (2013).
[4] M. L. Blow, S. P. Thampi, and J. M. Yeomans, Phys. Rev. Lett. **113**, 248303 (2014).
[5] L. Giomi, M. J. Bowick, P. Mishra, R. Sknepnek, and M. C. Marchetti, Philosophical Transactions of the Royal Society A: Mathematical, Physical and Engineering Sciences **372**, 20130365 (2014).
[6] S. P. Thampi, R. Golestanian, and J. M. Yeomans, Physical Review E **90**, 062307 (2014).
[7] S. P. Thampi, R. Golestanian, and J. M. Yeomans, Philosophical Transactions of the Royal Society A: Mathematical, Physical and Engineering Sciences **372**, 20130366 (2014).
[8] S. P. Thampi, R. Golestanian, and J. M. Yeomans, EPL (Europhysics Letters) **105**, 18001 (2014).
[9] H. H. Wensink, J. Dunkel, S. Heidenreich, K. Drescher, R. E. Goldstein, H. Lowen, and J. M. Yeomans, Proceedings of the National Academy of Sciences **109**, 14308 (2012), 1208.4239v1.
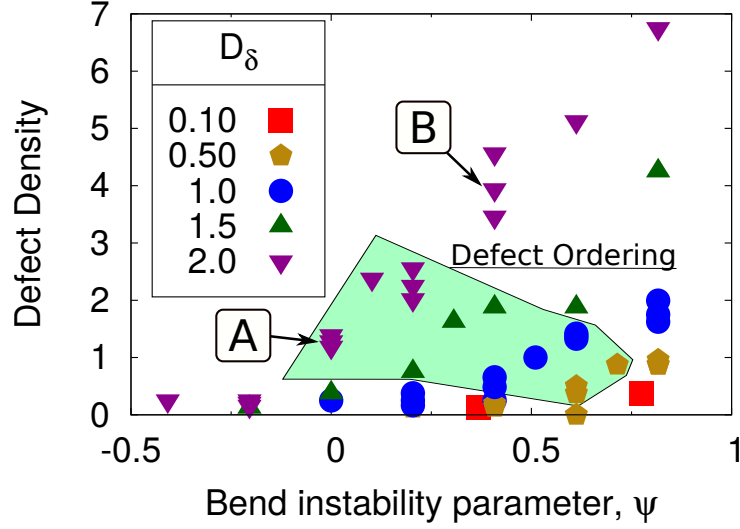
FIG. 2. This plot shows defect density (defects per $(100\ell_D)^2$), as a function of the bend instability parameter, below the bend instability ($\psi < 1$). The shaded region shows where $+\frac{1}{2}$ defects showed statistically significant polar ordering. This plot is a zoomed-in version of the plot on the left in Fig. 2 of the paper, and has parameters $\lambda_C = 1.0$, and $\rho_0 = 2.0$. The two points indicated are systems which are shown in Fig. 1 in the body of the paper. A is the defect-ordered state in the upper left, and B is the defective state below the bend instability, in the lower left.
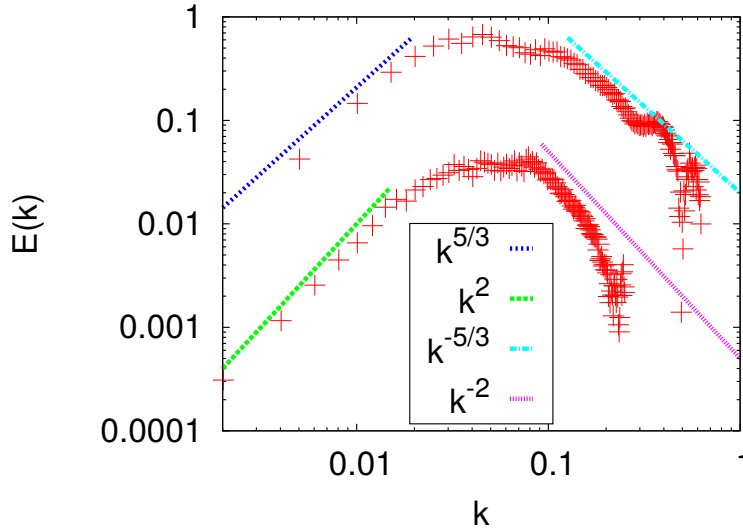


FIG. 3. Log-scale plots of the following approximation of the energy spectral density $E(k) = \frac{k}{2\pi} \int d^2 R e^{ik \cdot R} \langle \vec{v}(0) \cdot \vec{v}(R) \rangle$. Data shows two sets of parameters. Top: $(\rho_0, \lambda_R, D_\delta)=(2, 8, 1)$ and Bottom: $(3, 10, 0.5)$; scaled by multiplicative constants for comparison. The energy density seems to scale with a power laws of $k^{5/3}$ ($k^2$) for small wavevector, and $k^{-5/3}$ ($k^{-2}$) and for large wavevector for the upper (lower) curve. These u-shaped energy spectra are similar to what is seen in mixing flow in three dimensions, and is reminiscent of that seen in bacterial turbulence and a reversing-rod model [9].